Comparisons between 2D doubly vibrationally enhanced four wave mixing and site selective spectroscopy

ARTICLE *in* JOURNAL OF LUMINESCENCE · MAY 2000

Impact Factor: 2.72 · DOI: 10.1016/S0022-2313(99)00236-7

15 AUTHORS, INCLUDING:

Kent A Meyer
Oak Ridge National Laboratory
28 PUBLICATIONS **270** CITATIONS

SEE PROFILE

James P Hamilton
University of Wisconsin - Platteville
23 PUBLICATIONS **436** CITATIONS

SEE PROFILE

ELSEVIER

Journal of Luminescence 87–89 (2000) 90–95

JOURNAL OF LUMINESCENCE

www.elsevier.com/locate/jlumin

Invited Paper

Comparisons between 2D doubly vibrationally enhanced four wave mixing and site selective spectroscopy

Wei Zhao, Keith M. Murdoch, Nicholas J. Condon, Daniel M. Besemann, Kent A. Meyer, Peter C. Chen, James P. Hamilton, A. Zilian, Mitchell J. Labuda, David E. Thompson, Roger J. Carlson, Gregory B. Hurst, Michael T. Riebe, Jack K. Steehler, John C. Wright*

Department of Chemistry, University of Wisconsin, 1101 University Avenue, Madison, WI 53706, USA

Abstract

We have constructed a nonlinear spectroscopic system for performing multiresonant four-wave mixing with infrared lasers. The system consists of three coherent sources, two of which are tunable in the infrared region of the spectrum. The sources are tuned to different vibrational resonances and the four-wave mixing output is monitored as a function of the two infrared frequencies. When the frequencies match direct infrared absorption or Raman transitions, the four-wave mixing output is enhanced. A two-dimensional display of the data shows the output intensity as a function of the two infrared frequencies. We observe that cross-peaks appear in the 2D spectra when multiple resonances are excited. We have named the method "doubly vibrationally enhanced four-wave mixing (DOVE-FWM)". This method represents the long sought optical analogue to 2D nmr. It should provide a method that is complementary to nmr because of the difference in the time scales of the dephasing processes. Spin-lattice interactions fix the dephasing times for NMR measurements at millisecond time scales so nmr senses the ensemble average of a material's structure. Vibrational dephasing times occur on the picosecond time scale so the DOVE–FWM measurement represents a more instantaneous measurement of material structure.

Keywords: Four wave mixing; Nonlinear spectroscopy; Vibrational spectroscopy

1. Introduction

Laser-induced fluorescence spectroscopy is commonly used in luminescence spectroscopy to measure a material's properties. However, it fails when there is no luminescence. Nonlinear spectroscopic methods do not require luminescent emission because the output signal arises from a coherence, not an excited population that can be quenched. In this paper, we present a new family of multi-resonant nonlinear molecular spectroscopies and we show their relationship to current site selective laser methods that are important in luminescent materials. They are the optical analog to two-dimensional (2D) nuclear magnetic resonance (NMR). This new form of spectroscopy has a number of capabilities that promise to permit its application in many areas of science. These capabilities include the ability to narrow inhomogeneously broadened lines, remove spectral congestion, and isolate features that are associated with interactions between chromophores. The spectroscopies are also characterized by a fast time response that can freeze the dynamical information.

Site selective laser spectroscopy has played a key role for understanding the luminescent materials at an atomic and molecular level because it increases the spectral resolution. For example, it can narrow inhomogeneously broadened spectral lines and simplify the spectral congestion of a multi-component samples where each

*Corresponding author: Tel.: +1-608-262-0351; fax: +1-608-262-0453.

E-mail address: wright@chem.wisc.edu (J.C. Wright)

0022-2313/00/$ - see front matter
PII: S0022-2313(99)00236-7

component has its own spectrum. Site selective spectroscopy began with Szabo's demonstration of fluorescence line narrowing (FLN) in ruby [1] and was subsequently developed by Yen [2] who applied FLN to a variety of luminescent materials. Others extended it to molecular systems [3–5]. In FLN, a spectrally narrow laser excites a subset of chromophores within an inhomogeneously broadened band so the subsequent fluorescence is restricted to those sites that were excited, either by the initial excitation or later energy transfer. Subsequently, site selective spectroscopy was extended to complex materials with multiple sites. Here, a laser excited a chromophore in a particular site so only that site emitted fluorescence [6]. This technique was particularly helpful when the spectra were congested because of overlapping contributions from the multiple sites. All of these methods required fluorescence from the sample. We were particularly interested in developing the nonlinear analogues to these methods because the output signal in nonlinear spectroscopies is driven by the electric fields of the excitation lasers and are not subject to the same quenching interferences of fluorescence methods [7].

2. Background

In order to understand the relationships between site selective spectroscopy and nonlinear processes, we must first understand the nature of the fluorescence process that is central to site selective spectroscopy. Fig. 1a shows how the fluorescence process occurs using a Mukamel diagram [8] and a wave mixing (WM) diagram [9]. These diagrams are complementary because the Mukamel diagram shows the flow of coherence involved in a fluorescence process while the WM diagram shows the resonances with the states. A coherence occurs when an electromagnetic field induces a mixing of states so the linear superposition represents an oscillating time-dependent state that can be described by

$$\Psi(x,t) = c_a\psi_a(x)\,e^{i\omega_a t} + c_b\psi_b(x)\,e^{i\omega_b t}. \quad (1)$$

The coherence is proportional to a density matrix element, $\rho_{ba} \equiv c_a c_b^*$. The sequence of letters in the Mukamel diagram shows the evolution of the bra and ket portions of the coherence that are induced by an optical excitation with frequency ω_i. Thus, the notation aa → ba indicates a transition where a population in state a has evolved to a coherence given by ρ_{ba} because of interaction with a field at ω_i. Using this notation, fluorescence occurs through a four-wave mixing (FWM) interaction where field 1 induces a coherence, ρ_{ac}, which evolves to a coherence, ρ_{ab}, because of interaction with field 2. Field 2 can be an external field or it can be the vacuum field. If the field is external, the fluorescence is stimulated and if the field is from the vacuum, the fluorescence is spontaneous.

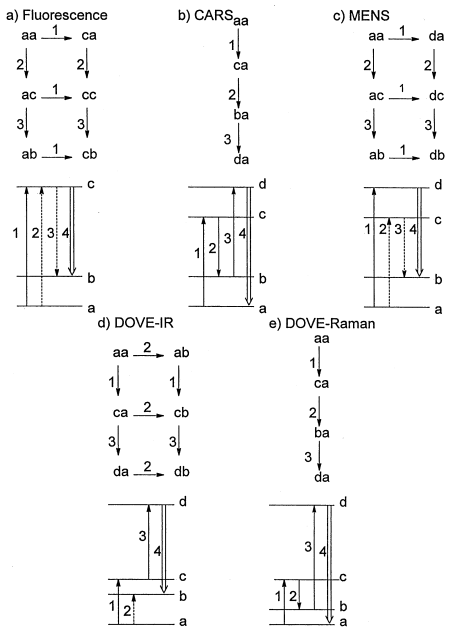

Fig. 1. This figure shows the Mukamel (top) and wave mixing diagrams (bottom) for five different processes. The Mukamel diagrams show the flow of coherences. Letters represent the bra and ket states in a coherence or population, i.e. the density matrices, arrows represent transitions between states, and numbers represent the laser frequencies. The wave mixing diagrams show the resonances. Solid arrows show transitions on the ket, dotted arrows show the transitions on the bra of the coherence, and double arrows show the output transition.

The evolution occurs only on the bra part of the coherence. Field 3 causes evolution on the ket side when state a makes a transition to state c. After these three interactions, the coherence becomes ρ_{cb} and so the system is left in a superposition state, i.e. a mixture of states c and b. Such a state is time dependent and oscillates at the frequency difference between the two states. The oscillation results in the light radiation that is detected.

There are different time orderings for these interactions and they are responsible for different processes. Fluorescence occurs for the time orderings aa → ac → cc → cb or aa → ca → cc → cb and, in both cases, there is an intermediate population that can be quenched. There is a third time ordering, aa → ac → ab → cb, that does not involve an intermediate population and contains the contribution to Raman scattering. (It also contains a contribution to fluorescence that interferes with the first two pathways.) Although Raman scattering could also be used for site selective spectroscopy, it has found limited application. Both fluorescence and Raman processes are examples of nonparametric processes. Nonparametric processes involve changes in both states represented by a coherence and the system is left in a different state at

the end of the process. Parametric processes involve changes in one state and the system returns to the initial state at the end of the process.

Four-wave mixing nonlinear spectroscopy also uses three interactions to launch the fourth output wave [7]. All three electromagnetic waves are furnished by coherent sources without contributions from the vacuum. The most common nonlinear method is coherent anti-Stokes Raman spectroscopy (CARS). Fig. 1b shows its coherence evolution and the resonances. Since each of the interactions can be resonant, site selective spectroscopy is possible with CARS if the resonances enhance the contributions from specific sites. FWM is measured by the third order susceptibility, $\chi^{(3)}$, which is the proportionality constant between the electric field and the induced polarization. The frequency dependence of $\chi^{(3)}$ for CARS is given by the expression:

$$\chi^{(3)} = \frac{A}{(\omega_{ca} - \omega_1 - i\Gamma_{ca})(\omega_{ba} - \omega_1 + \omega_2 - i\Gamma_{ba})(\omega_{da} - \omega_4 - i\Gamma_{da})}. \quad (2)$$

where A controls the magnitude of $\chi^{(3)}$, ω_{ij} and Γ_{ij} are the frequency and dephasing rate of the $i \Leftrightarrow j$ transition, ω_1 is a laser frequency, and $\omega_4 = \omega_1 - \omega_2 + \omega_3$ is the output frequency. CARS is an example of a parametric process where the system returns to state a.

CARS is contrasted with a multiply enhanced nonparametric spectroscopy (MENS) nonlinear method shown in Fig. 1c [10–12]. It has Raman resonances that are analogous to CARS but it has the multiple pathways characteristic of a nonparametric process. For MENS, the frequency dependence of $\chi^{(3)}$ is given by the expression:

$$\chi^{(3)} = A\left(\frac{1}{(\omega_{da} - \omega_1 - i\Gamma_{da})(\omega_{dc} - \omega_1 + \omega_2 - i\Gamma_{dc})(\omega_{db} - \omega_4 - i\Gamma_{db})} - \frac{1}{(\omega_{ca} - \omega_2 + i\Gamma_{ca})(\omega_{dc} - \omega_1 + \omega_2 - i\Gamma_{dc})(\omega_{db} - \omega_4 - i\Gamma_{db})} + \frac{1}{(\omega_{ca} - \omega_2 + i\Gamma_{ca})(\omega_{ba} - \omega_2 + \omega_3 - i\Gamma_{ba})(\omega_{db} - \omega_4 - i\Gamma_{db})}\right). \quad (3)$$

There are three terms because there are three pathways by which the initial ground state population given by ρ_{aa} evolves to the final coherence ρ_{db}. This form is somewhat misleading, however, because in the absence of pure dephasing events, there are interference effects between the terms that can hide some of the resonances. One can show that the terms can be combined into a much simpler form:

$$\chi^{(3)} = \frac{A}{(\omega_{da} - \omega_1 - i\Gamma_{da})(\omega_{ca} - \omega_2 + i\Gamma_{ca})(\omega_{ba} - \omega_2 + \omega_3 + i\Gamma_{ba})}. \quad (4)$$

Note first that MENS also has three resonances but in addition, the relative signs for the real and imaginary parts of the denominator are different between Eqs. (2) and (4). This difference is important for determining the line shapes of resonances and the line narrowing of nonlinear processes.

In order to perform site selective spectroscopy, the excitation sources are tuned to one or even two resonances of a particular chromophore in a particular site while another resonance is scanned. Site selective occurs because the sites or chromophores that are multiply resonant are multiplicatively enhanced so their features are much brighter than those that have fewer resonances [11–13].

Line narrowing can be achieved when the resonant sites within an inhomogeneous distribution of sites dominate the output spectrum. There is an important subtlety though because even though a site is multiplicatively resonant and is therefore strongly enhanced, there are many more nearly resonant sites. Since FWM is a coherent process, the contributions from all sites and chromophores add and interfere, either constructively or destructively. The net effect requires that one perform the

ensemble average over all the contributions within the inhomogeneous distribution. When this average is performed, it is found that parametric and nonparametric nonlinear processes differ in whether constructive or destructive interference occurs between components, depending upon how the inhomogeneous broadening effects shift the different resonant states [14–17]. If it shifts their energies in the same direction, parametric processes like CARS have destructive interference between the resonant sites and the more numerous nearly resonant sites. The resonant site contribution is suppressed so it cannot make a dominant contribution to the spectrum. No line narrowing is observed. However, nonparametric processes like MENS have constructive interference so the narrowing can be observed.

In addition to site selection, there are also vibrational mode selection effects that become important in determining whether multiple resonances are multiplicatively enhanced. For example, if two resonances occur with different vibrational modes, the evolution of the coherence will require transitions involving state changes in both modes. These changes cannot occur if the modes are uncoupled. Intuitively, multiple enhancements occur when the lasers drive a resonance that causes a modulation in the states associated with a second resonance. Since the coupling of two modes requires interactions, the mode selectivity allows one to isolate the mode pairs involved in the interactions.

These ideas were implemented using the sharp lines that are characteristic of rigid organic chromophores such as pentacene. Three tunable lasers are tuned to achieve triple resonance involving the pentacene excited electronic state, a vibrational state of the ground electronic state, and a vibronic state of the excited electronic state. The component selection [11–13], line narrowing [18–22], and mode selection [23–26] capabilities of CARS and MENS where demonstrated at cryogenic temperatures where the pentacene transitions are sharp and spectral selectivity is possible.

Although this selectivity is achievable at low temperatures, it is important to extend these methods to probe molecular systems at room temperature. Vibrational transitions have sharp lines at room temperatures because the vibrational states are not perturbed by thermal fluctuations as strongly as electronic transitions. However, the nonlinearities of vibrational transitions are inherently much weaker than electronic transitions. Optical nonlinearities are caused by interactions between two or more polarizations that are induced by two or more optical electric fields. Since the electrons in molecules are so much lighter than the nuclei, the induced polarization is dominated by the electron polarization and the nuclear polarization is usually negligible. The key to achieving nonlinear vibrational spectroscopy lies in increasing the nuclear polarization by tuning the excitation to resonance.

There are two forms of nonlinear vibrational FWM that are particularly promising for providing doubly vibrationally enhanced (DOVE) spectra-DOVE IR FWM and DOVE-Raman FWM [27–31]. The diagrams for both processes are shown in Fig. 1d and e. One can see that they are very similar to MENS and CARS. The only difference is their dependence on vibrational transitions. DOVE IR is a nonparametric process while DOVE-Raman is a parametric process. One can show that, in the absence of pure dephasing, the frequency dependence of $\chi^{(3)}$ for DOVE IR and DOVE Raman are

$$\chi^{(3)} = \frac{A}{(\omega_{ca} - \omega_1 - i\Gamma_{ca})(\omega_{baa} - \omega_2 + i\Gamma_{ba})(\omega_{db} - \omega_4 - i\Gamma_{db})} \quad (5)$$

and

$$\chi^{(3)} = \frac{A}{(\omega_{ca} - \omega_1 - i\Gamma_{ca})(\omega_{ba} - \omega_1 + \omega_2 + i\Gamma_{ba})(\omega_{db} - \omega_4 - i\Gamma_{da})}, \quad (6)$$

respectively. These equations show that DOVE-IR and DOVE-Raman have a different dependence on the ω_1 and ω_2 frequencies and these differences serve as signatures for the processes.

3. Results

These processes were implemented using a mode-locked Nd : YAG laser to excite two optical parametric oscillators/amplifiers (OPO/OPA) that can provide tunable infrared light at ω_1 and ω_2. The Nd : YAG laser provides the last field at ω_3. These three beams are focused into a sample at the angles required for optimal phase matching. The sample was a 35 : 1 mole : mole mixture of acetonitrile and deuterobenzene. The deuterobenzene was present as an internal standard so accurate values of $\chi^{(3)}$ could be obtained from the data. The output beam at ω_4 was isolated with apertures,

a monochromator, and measured with a photomultiplier as a function of ω_1 and ω_2. Fig. 2 shows a representative FWM spectra for different values of ω_2 while ω_1 was scanned and the FWM intensity at ω_4 was monitored. A more complete description is published elsewhere [32,33]. It is clear that the spectrum changes dramatically depending on the choice of the ω_2 frequency.

The spectra are determined by the vibrational absorption and Raman spectra [32,33]. Deuterobenzene has a strong Raman transition at $\omega_1 - \omega_2 = 944\ \mathrm{cm}^{-1}$. Acetonitrile has a Raman transition from the ν_4 C–C stretch at $918\ \mathrm{cm}^{-1}$ and infrared absorption lines from the ν_2 C ≡ N stretch mode at $\omega_2 = 2253\ \mathrm{cm}^{-1}$ and from the $\nu_2 + \nu_4$ combination band at $\omega_1 = 3163\ \mathrm{cm}^{-1}$. Fig. 2 can be best interpreted by realizing that the spectrum with $\omega_2 = 2500\ \mathrm{cm}^{-1}$ corresponds to a region where there are no strong absorption features and therefore double resonances are not possible. Only two lines are seen in this spectrum, one from the $\omega_1 - \omega_2 = 918\ \mathrm{cm}^{-1}$ and the other from the $944\ \mathrm{cm}^{-1}$ Raman transition. Since the $944\ \mathrm{cm}^{-1}$ line is so much stronger than the $918\ \mathrm{cm}^{-1}$ line, it can still be comparable in intensity despite the low deuterobenzene concentration. These two Raman features have the same relative intensity if there are no additional nonlinear processes. However, as can be seen from the $\omega_2 = 2253\ \mathrm{cm}^{-1}$ spectrum, other processes do occur. In particular, there is a very strong peak at $\omega_1 = 3363\ \mathrm{cm}^{-1}$ for the $\omega_2 = 2253\ \mathrm{cm}^{-1}$ spectrum. It is clear that the peak represents a double resonance because it diminishes in intensity when ω_2 moves off the $2253\ \mathrm{cm}^{-1}$ resonance. The two Raman lines are not seen in this spectrum because they are too weak compared with the double resonance peak. The spectra for $\omega_2 = 2262$ and $2266\ \mathrm{cm}^{-1}$ show how the Raman lines return when ω_2 is detuned. This spectral behavior is the signature of a DOVE feature.

The mode selection capabilities are demonstrated by examining other pairs of vibrational modes to see if there are cross-peaks. These experiments are being reported elsewhere [34]. It is important to realize that double resonance peaks can only occur when the two vibrational states are coupled by an intra- or intermolecular interaction [35–39]. If there is no coupling because the vibrational modes do not involve common states, there can be no doubly resonant peak.

In order to test the mode selectivity, we examined the acetonitrile spectra for double resonance features in the neighborhood of the acetonitrile C–H stretch mode and C ≡ N stretch mode and found there was no observable cross-peak. The C–H and the C ≡ N in acetonitrile (CH_3CN) are separated from each other by a C–C bond which reduces any coupling. The double resonance feature that is observed is caused by the coupling between the C ≡ N and C–C bonds which are adjacent to each other so excitation of one causes a modulation of the electron density in the other bond. A combination band

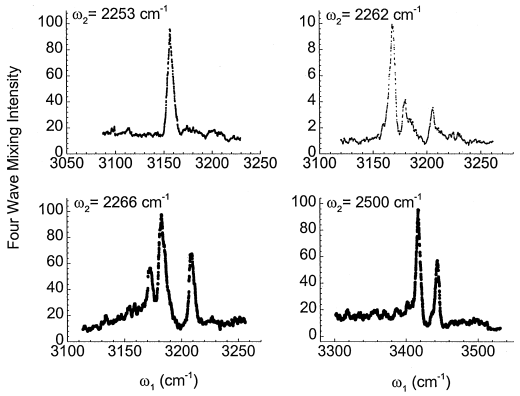

Fig. 2. Representative DOVE-FWM spectra of acetonitrile/deuterobenzene mixture where ω_1 is scanned and ω_2 is set for the different values shown in the figure.

appears in the normal infrared absorption spectrum as a result. The DOVE-IR feature can now appear because there is a mechanism to have transitions involving two separate modes. If we designate the number of vibrational quanta associated with vibrational modes ν_2 and ν_4 by the notation, (i, j), respectively, the transitions associated with the DOVE-IR feature become $(0,0) \rightarrow (1,1)$ for the infrared absorption combination band, $(0,0) \rightarrow (1,0)$ for the infrared absorption involving ν_2, and $(1,1) \rightarrow (1,0)$ for the Raman transition. Each of the DOVE-IR transitions involves single-vibrational quantum changes that do not involve coupling, except for the combination band transition where two vibrational quanta change.

The component selectivity was demonstrated by using a mixture of acetonitrile and deuteroacetonitrile and is published elsewhere [33]. The deuteration shifts the ν_2 frequency by $9\ \mathrm{cm}^{-1}$ so it is possible to set ω_2 for resonance with either the acetonitrile or deuteroacetonitrile ν_2 modes and scan ω_1 over the region of the combination bands. When this experiment was performed, we observed only the DOVE feature from the component that was chosen for resonance with ω_1. If ω_2 was set between the two frequencies, we observed only weak features from both components.

The line narrowing capabilities of DOVE-IR were demonstrated by using a mixture of acetonitrile and water and are described elsewhere [40]. Water is a strongly hydrogen bonding solvent and the diversity of hydrogen bonds that form with the acetonitrile cause broadening of the vibrational transitions. When the same DOVE experiments were performed on these samples, we observed that the DOVE vibrational features were narrower than the corresponding infrared absorption lines. More importantly, the position of the lines shifted in the spectrum as ω_2 was moved to different positions within the inhomogeneously broadened envelope of the

v_2 mode. We interpret this shifting as the site selection of acetonitrile in different hydrogen bonding environments. If hydrogen bonding shifts the v_2 and $(v_2 + v_4)$ transitions in the same direction, establishing a resonance with a particular value of ω_2 will result in shifted peaks when ω_1 is scanned.

4. Conclusions

This work demonstrates the feasibility for a new approach to site selective spectroscopy that is based on nonlinear interactions and is free from quenching influences. We have shown that the approach is capable of line narrowing, component selection, and mode selection. Although the approach was demonstrated for molecular spectroscopy, it is applicable in all the situations where spectroscopy is used. In particular, the mode selection ideas are more general than the applications to molecular spectroscopy suggests. The essence of the approach is to use multiple resonances with different states to achieve spectral selectivity. These multiple resonances will not appear without interactions that couple the states. Thus, the nonlinear methods can provide spectra that selectively enhance multiresonant features that are associated with interactions. Since these interactions are usually central to application questions in developing new technologies, we believe that the new methods will become important in many fields of science, including luminescence spectroscopy.

Acknowledgements

This work was supported by the Chemistry Program of the National Science Foundation under grant CHE-9816829.

References

[1] A. Szabo, Phys. Rev. Lett. 25 (1970) 924.
[2] R. Flach, D.S. Hamilton, P.M. Selzer, W.M. Yen, Phys. Rev. Lett. 35 (1975) 1034.
[3] J.H. Everly, W.C. McColgin, K. Kawaoka, A.P. Marchetti, Nature 251 (1974) 215.
[4] A.P. Marchetti, W.C. McColgin, J.H. Eberly, Phys. Rev. Lett. 35 (1975) 387.
[5] J.C. Brown, M.C. Edelson, G.J. Small, Anal. Chem. 50 (1978) 1394.
[6] D.R. Tallant, J.C. Wright, J. Chem. Phys. 63 (1975) 2075.
[7] J.C. Wright et al., Int. Rev. Phys. Chem. 10 (1991) 349.
[8] S. Mukamel, Principles of Nonlinear Optical Spectrscopy, 1st Edition, Oxford University Press, New York, 1995.
[9] D. Lee, A.C. Albrecht, Advances in Infrared and Raman Spectroscopy, Vol. 12, 1st Edition, Wiley, Chichester, 1985.
[10] D.C. Nguyen, J.C. Wright, Chem. Phys. Lett. 117 (1985) 224.
[11] J.K. Steehler, J.C. Wright, J. Chem. Phys. 83 (1985) 3200.
[12] S.H. Lee, J.K. Steehler, D.C. Nguyen, J.C. Wright, Appl. Spectrosc. 39 (1985) 243.
[13] J.K. Steehler, J.C. Wright, Chem. Phys. Lett. 115 (1985) 486.
[14] S.A.J. Druet, J.P.E. Taran, C.J. Borde, J. Phys. 40 (1979) 819.
[15] F. Ouellette, M.M. Denariez-Roberge, Can. J. Phys. 60 (1982) 877.
[16] F. Ouellette, M.M. Denariez-Roberge, Can. J. Phys. 60 (1982) 1477.
[17] J.L. Oudar, Y.R. Shen, Phys. Rev. A 22 (1980) 1141.
[18] M.T. Riebe, J.C. Wright, Chem. Phys. Lett 138 (1987) 565.
[19] M.T. Riebe, J.C. Wright, J. Chem. Phys. 88 (1988) 2981.
[20] G.B. Hurst, J.C. Wright, J. Chem. Phys. 95 (1991) 1479.
[21] G.B. Hurst, J.C. Wright, J. Chem. Phys. 97 (1992) 3940.
[22] T.C. Chang, C.K. Johnson, G.J. Small, J. Phys. Chem. 89 (1985) 2984.
[23] R.J. Carlson, D.C. Nguyen, J.C. Wright, J. Chem. Phys. 92 (1990) 1538.
[24] R.J. Carlson, J.C. Wright, J. Chem. Phys. 92 (1990) 5186.
[25] R.J. Carlson, J.C. Wright, J. Chem. Phys. 93 (1990) 2205.
[26] R.J. Carlson, J.C. Wright, Anal. Chem. 63 (1991) 1449.
[27] A. Zilian, M.J. LaBuda, J.P. Hamilton, J.C. Wright, J. Lumin. 60&61 (1994) 655.
[28] A. Zilian, M.J. LaBuda, J.P. Hamilton, J.C. Wright, J. Lumin. 60&61 (1994) 410.
[29] J.C. Wright et al., Appl. Spectrosc. 51 (1997) 949.
[30] P.C. Chen et al., Appl. Spectrosc. 52 (1998) 380.
[31] J.C. Wright et al., J. Lumin. 72–74 (1997) 799.
[32] W. Zhao, J.C. Wright, Phys. Rev. Lett. 83 (1999) 1950.
[33] W. Zhao, J.C. Wright, Phys. Rev. Lett. 84 (2000) 1411.
[34] W. Zhao, J.C. Wright, J. Am. Chem. Soc. 121 (1999) 10994.
[35] K. Okumura, Y. Tanimura, J. Chem. Phys. 106 (1997) 1687.
[36] Y. Tanimura, K. Okumura, J. Chem. Phys. 106 (1997) 2078.
[37] K. Okumura, Y. Tanimura, J. Chem. Phys. 107 (1997) 2267.
[38] V. Chernyak, S. Mukamel, J. Chem. Phys. 108 (1998) 5812.
[39] M. Cho, K. Okumura, Y. Tanimura, J. Chem. Phys. 108 (1998) 1326.
[40] D. Besemann, W. Zhao, J.C. Wright, Phys. Rev. Lett., to be published.